Benchmarking theoretical formalisms for (p,pn) reactions: The ^{15}C$(p,pn)^{14}$C case

K. Yoshida,[1,*] M. Gómez-Ramos,[2] K. Ogata,[1] and A. M. Moro[2]
[1]*Research Center for Nuclear Physics (RCNP), Osaka University, Ibaraki 567-0047, Japan*
[2]*Departamento de FAMN, Universidad de Sevilla, Apartado 1065, 41080 Sevilla, Spain*

(Received 13 November 2017; published 12 February 2018)

Background: Proton-induced knockout reactions of the form (p,pN) have experienced a renewed interest in recent years due to the possibility of performing these measurements with rare isotopes, using inverse kinematics. Several theoretical models are being used for the interpretation of these new data, such as the distorted-wave impulse approximation (DWIA), the transition amplitude formulation of the Faddeev equations due to Alt, Grassberger, and Sandhas (FAGS) and, more recently, a coupled-channels method here referred to as transfer-to-the-continuum (TC).
Purpose: Our goal is to compare the momentum distributions calculated with the DWIA and TC models for the same reactions, using whenever possible the same inputs (e.g., distorting potential). A comparison with already published results for the FAGS formalism is performed as well.
Method: We choose the ^{15}C$(p,pn)^{14}$C reaction at an incident energy of 420 MeV/u, which has been previously studied with the FAGS formalism. The knocked-out neutron is assumed to be in a $2s$ single-particle orbital. Longitudinal and transverse momentum distributions are calculated for different assumed separation energies.
Results: For all cases considered, we find a very good agreement between DWIA and TC results. The energy dependence of the distorting optical potentials is found to affect in a modest way the shape and magnitude of the momentum distributions. Moreover, when relativistic kinematics corrections are omitted, our calculations reproduce remarkably well the FAGS result.
Conclusions: The results found in this work provide confidence on the consistency and accuracy of the DWIA and TC models for analyzing momentum distributions for (p,pn) reactions at intermediate energies.

DOI: 10.1103/PhysRevC.97.024608

I. INTRODUCTION

Thanks to the development of radioactive isotope beam technology, experiments on unstable nuclei in inverse kinematics have been made possible. Among them, studies on single-particle structure and its evolution in nuclei away from the stability valley is one of the main subjects of study in present day nuclear physics. Knockout reactions induced by intermediate energy protons have been one of the most successful tools for studying the single-particle nature both of stable and unstable nuclei. The distorted-wave impulse approximation (DWIA) is one of the reaction models which has been successfully applied to the analysis of these reactions [1–6] (for a recent review, see Ref. [7]). Most DWIA applications have been done for exclusive measurements and under *quasifree* scattering conditions. It remains to assess the accuracy of the method for more inclusive observables, such as total nucleon removal cross sections and momentum distributions of the residual heavy fragment. A recent step toward this goal is provided by the eikonal DWIA formalism recently proposed in Ref. [8].

In recent years, the Alt-Grassberger-Sandhas formulation of the Faddeev equations (FAGS) [9,10], which uses a momentum-space representation of the scattering transition amplitude, has been put forward as an alternative for the analysis of these kinds of processes [11–14].

Very recently, another reaction model, referred to as the transfer-to-the-continuum (TC) framework, has been developed and applied to (p,pN) reactions [15,16]. Since these three formalisms are being used to analyze experimental data, it is of timely importance to establish the consistency among them, and understand the limitations and range of validity in each case.

Within the same scope, it has been shown in [11,12] that one can recover the DWIA formalism using a truncated Faddeev multiple-scattering series. However, the DWIA so obtained differs in some aspects from the one commonly used in actual analyses of (p,pN) data, since the latter usually involves additional approximations.

It is therefore essential to make a comparison between these models and, as a first step towards this goal, in this paper we make a benchmark comparison between DWIA, TC, and FAGS, for a given (p,pn) reaction using, whenever possible, the same input ingredients in the calculations.

The content of the paper is as follows. In Sec. II the formulation of the DWIA and the TC formalisms is given. In Sec. III the longitudinal momentum distributions (LMDs) of the ^{15}C$(p,pn)^{14}$C reaction with DWIA an TC are compared, for different separation energies and studying the effect of the energy dependence of the distorting potentials for the emitted nucleons. A comparison with the FAGS transversal momentum distributions (TMDs) published in Ref. [14] is also presented. Finally, the summary is given in Sec. IV.

*yoshidak@rcnp.osaka-u.ac.jp

II. FORMALISM

We consider A(p,pn)B knockout reaction in inverse kinematics. Observables shown below with superscript A are evaluated in the so-called A-rest frame.

A. DWIA framework

In the DWIA formalism, the transition amplitude for a A(p,pn)B reaction is given by

$$T^{nljm}_{\boldsymbol{K}_0\boldsymbol{K}_1\boldsymbol{K}_2} = \left\langle \chi^{(-)}_{1,\boldsymbol{K}_1}\chi^{(-)}_{2,\boldsymbol{K}_2} \,\middle|\, t_{pn} \,\middle|\, \chi^{(+)}_{0,\boldsymbol{K}_0}\varphi^{nljm}\right\rangle, \tag{1}$$

where χ_0, χ_1, and χ_2 are the scattering wave functions of the p-A, p-B, and n-B systems, respectively, φ^{nljm} is the single-particle wave function with n, l, j, and m being the principal quantum number, the orbital angular momentum, the total angular momentum, and its third component of n bound in A, respectively. The transition interaction t_{pn} is the effective interaction between p-n pair which reproduces p-n binary scattering.

By applying the so-called factorization approximation, which has been reconfirmed to be valid in Ref. [17], Eq. (1) is reduced to

$$T^{nljm}_{\boldsymbol{K}_0\boldsymbol{K}_1\boldsymbol{K}_2} \approx \langle \boldsymbol{\kappa}' \,|\, t_{pn} \,|\, \boldsymbol{\kappa}\rangle \int d\boldsymbol{R}\, F(\boldsymbol{R})\varphi^{nljm}(\boldsymbol{R}), \tag{2}$$

where $F(\boldsymbol{R})$ is defined by

$$F(\boldsymbol{R}) \equiv \chi^{*(-)}_{1,\boldsymbol{K}_1}(\boldsymbol{R})\,\chi^{*(-)}_{2,\boldsymbol{K}_2}(\boldsymbol{R})\,\chi^{(+)}_{0,\boldsymbol{K}_0}(\boldsymbol{R})\,e^{-i\boldsymbol{K}_0\cdot\boldsymbol{R}/A}. \tag{3}$$

The initial and final relative momenta of the p-n system are defined by

$$\boldsymbol{\kappa} \equiv (\alpha_0\boldsymbol{K}_0 - \boldsymbol{K}_n)/2, \tag{4}$$

$$\boldsymbol{\kappa}' \equiv (\boldsymbol{K}_1 - \boldsymbol{K}_2)/2 \tag{5}$$

with $\alpha_0 = (A+1)/A$. The momentum of n in the initial state $\boldsymbol{K}_n$ is evaluated from asymptotic momenta by assuming the momentum conservation in the p-n system:

$$\boldsymbol{K}_n = \boldsymbol{K}_1 + \boldsymbol{K}_2 - \alpha_0\boldsymbol{K}_0. \tag{6}$$

In the present study on-the-energy-shell (on-shell) approximation is adopted in taking the squared modulus of Eq. (2):

$$\frac{\mu^2_{pn}}{(2\pi\hbar^2)^2}|\langle \boldsymbol{\kappa}' \,|\, t_{pn} \,|\, \boldsymbol{\kappa}\rangle|^2 \approx \frac{d\sigma_{pn}}{d\Omega_{pn}}(E_{pn},\theta_{pn}), \tag{7}$$

where μ_{pn} is the reduced mass of the p-n system, θ_{pn} is the angle between $\boldsymbol{\kappa}'$ and $\boldsymbol{\kappa}$, and the p-n scattering energy is given by

$$E_{pn} = \frac{\hbar^2(\kappa^2+\kappa'^2)/2}{2\mu_{pn}}. \tag{8}$$

In the present DWIA, the momentum distribution (MD) is given by

$$\frac{d\sigma}{d\boldsymbol{K}^{\rm A}_{\rm B}} = C_0 \int d\boldsymbol{K}^{\rm A}_1 d\boldsymbol{K}^{\rm A}_2 \eta^{\rm A}_{{\rm M}\phi{\rm l}}\delta\left(E^{\rm A}_f - E^{\rm A}_i\right)\delta\left(\boldsymbol{K}^{\rm A}_f - \boldsymbol{K}^{\rm A}_i\right) \times \frac{d\sigma_{pn}}{d\Omega_{pn}}(E_{pn},\theta_{pn})\sum_m (2\pi)^2\left|\bar{T}^{nljm}_{\boldsymbol{K}_0\boldsymbol{K}_1\boldsymbol{K}_2}\right|^2, \tag{9}$$

where

$$C_0 \equiv \frac{E^{\rm A}_0}{(\hbar c)^2 K^{\rm A}_0}\frac{1}{(2l+1)}\frac{\hbar^4}{(2\pi)^3\mu^2_{pn}}, \tag{10}$$

$$\eta^{\rm A}_{{\rm M}\phi{\rm l}} \equiv \frac{E_1E_2E_{\rm B}}{E^{\rm A}_1E^{\rm A}_2E^{\rm A}_{\rm B}}, \tag{11}$$

and the reduced transition amplitude is given by

$$\bar{T}^{nljm}_{\boldsymbol{K}_0\boldsymbol{K}_1\boldsymbol{K}_2} = \int d\boldsymbol{R}\, F(\boldsymbol{R})\varphi^{nljm}(\boldsymbol{R}). \tag{12}$$

Longitudinal and transverse MD are obtained from MD as follows:

$$\frac{d\sigma}{dK^{\rm A}_{{\rm B}z}} = 2\pi\int dK^{\rm A}_{{\rm B}b}K^{\rm A}_{{\rm B}b}\frac{d\sigma}{d\boldsymbol{K}^{\rm A}_{\rm B}}, \tag{13}$$

$$\frac{d\sigma}{dK^{\rm A}_{{\rm B}x}} = \int dK^{\rm A}_{{\rm B}y}dK^{\rm A}_{{\rm B}z}\frac{d\sigma}{d\boldsymbol{K}^{\rm A}_{\rm B}}. \tag{14}$$

B. Transfer to the continuum model

The transfer to the continuum formalism is based on the prior representation of the transition matrix for the A(p,pn)B process:

$$T^{nljm}_{\rm if} = \left\langle \Psi^{3b(-)}_f \,\middle|\, V_{pn} + V_{p{\rm B}} - U_{p{\rm A}} \,\middle|\, \chi^{(+)}_{0,\boldsymbol{K}_0}\varphi^{nljm}\right\rangle, \tag{15}$$

where φ^{nljm} and $\chi^{(+)}_{0,\boldsymbol{K}_0}$ are defined as above, V_{pn} and $V_{p{\rm B}}$ are the corresponding binary potentials, $U_{p{\rm A}}$ is the optical potential used to generate the distorted wave $\chi^{(+)}_{0,\boldsymbol{K}_0}$, and $\Psi^{3b(-)}_f$ is the final state wave function, which is formally treated as a three-body wave function, under the approximation that the state of B is not modified during the reaction.

In order to perform the calculation, $\Psi^{3b(-)}_f$ is expanded in terms of $p+n$ eigenstates, that is,

$$\Psi^{3b(-)}_f(\mathbf{r},\mathbf{R}) = \sum_{j'\pi}\int dk\phi^{j'\pi}(k,\mathbf{r})\chi^{j'\pi}(\mathbf{K},\mathbf{R}), \tag{16}$$

where k is the relative wave number of the $p+n$ pair and K is the wave number for the relative motion between B and the $p+n$ pair and is related to k through energy conservation. $\phi^{j'\pi}(k,\mathbf{r})$ are the eigenstates for the $p+n$ Hamiltonian with the interaction V_{pn} and wave number k, total angular momentum j and parity π while $\chi^{j'\pi}(\mathbf{K},\mathbf{R})$ describes the motion of the $p+n$ pair with respect to B for a wave number K, with the $p+n$ pair having total momentum j and parity π. Note that the expansion (16) contains also the term with the bound deuteron. This term is omitted here for brevity.

The k continuum is discretized using a binning procedure in a similar way to continuum-discretized coupled-channel calculations (CDCC),

$$\Psi^{3b(-)}_f(\mathbf{r},\mathbf{R}) \approx \sum_{Nj'\pi}\phi^{j'\pi}_N(k_N,\mathbf{r})\chi^{j'\pi}_N(\mathbf{K}_N,\mathbf{R}), \tag{17}$$

where k_N is an average momentum of the bin, and ϕ_N are the bin wave functions. As such, the transition matrix results in

$$T_{\rm if} \approx \sum_{Nj'\pi} \langle \phi_N^{j'\pi} \chi_N^{j'\pi} | V_{pn} + V_{p\rm B} - U_{p\rm A} | \chi^{(+)}_{0,\boldsymbol{K}_0} \varphi^{nljm} \rangle. \quad (18)$$

In order to make a more meaningful comparison with the DWIA calculations, the terms $V_{p\rm B} - U_{p\rm A}$ have been ignored, in what is called the *no-remnant* approximation,

$$T_{\rm if} \approx \sum_{Nj'\pi} \langle \phi_N^{j'\pi} \chi_N^{j'\pi} \mid V_{pn} \mid \chi^{(+)}_{0,\boldsymbol{K}_0} \varphi^{nljm} \rangle. \quad (19)$$

This transition amplitude is computed employing a calculation akin to a coupled-channel Born approximation (CCBA), from which the angular differential cross section to each of the bin states can be computed. A double differential cross section on the outgoing angle of B and the internal energy of the $p+n$ pair can be obtained from the angular differential cross section to each of the bins through

$$\left.\frac{{\rm d}^2\sigma_{j'\pi}}{{\rm d}\epsilon_{pn}{\rm d}\Omega_B}\right|_{\epsilon_{pn}\in\Delta_N} \approx \frac{1}{\Delta_N}\frac{{\rm d}\sigma_{N,j'\pi}}{{\rm d}\Omega_B}, \quad (20)$$

where Δ_N is the energy width of the bin $\{N, j', \pi\}$. Through energy conservation and the proper Jacobians, the longitudinal and transverse momentum distributions of B can be obtained from this double differential cross section.

From the practical point of view, an appealing feature of the TC method is that the sum in Eqs. (17)–(19) converges with a few values of j' (typically $j < 4$ at the intermediate energies considered here). A limitation is however that the interactions p+B and n+B are assumed to be energy independent. The accuracy of this will be investigated in the next section by comparing with the DWIA calculations.

The transfer to the continuum calculations have been performed using a modified version of the code FRESCO [18]. Further details can be found in [15].

III. RESULTS AND DISCUSSION

In this section, we compare the calculations with the TC and DWIA methods described in the preceding section. We consider the reaction ^{15}C$(p,pn)^{14}$C, calculating the knockout of a neutron in a $2s$ single-particle orbital and for three different separation energies: $S_n = 1.22$ MeV (i.e., the physical value), 5 MeV and 18 MeV.

A. Numerical inputs

The single-particle wave function of the struck neutron, φ^{nljm}, is obtained for a Woods-Saxon central potential $V(R) = V_0/(1+\exp[(R - r_0 B^{1/3})/a_0])$ with $r_0 = 1.25$ fm and $a_0 = 0.65$ fm. The depth parameter V_0 is adjusted so as to give neutron separation energies $S_n = 1.22$ MeV, 5 MeV, and 18 MeV.

For the nucleon-nucleon interaction, we employ the Reid93 potential [19], a generalized version of the pioneering Reid soft core potential [20], developed by the Nijmegen group. This potential contains central, spin-orbit and tensor components, and reproduces accurately the proton-proton and proton-neutron phase-shifts up to an energy of 350 MeV ($\chi^2/N_{\rm data} = 1.03$).

As for the distorting potential of p-A, p-B, and n-B systems, we use the EDAD2 parameter set of the Dirac phenomenology [21]. In the comparison with the FAGS calculations, the global optical potential parameters of Koning and Delaroche [22] will be also considered.

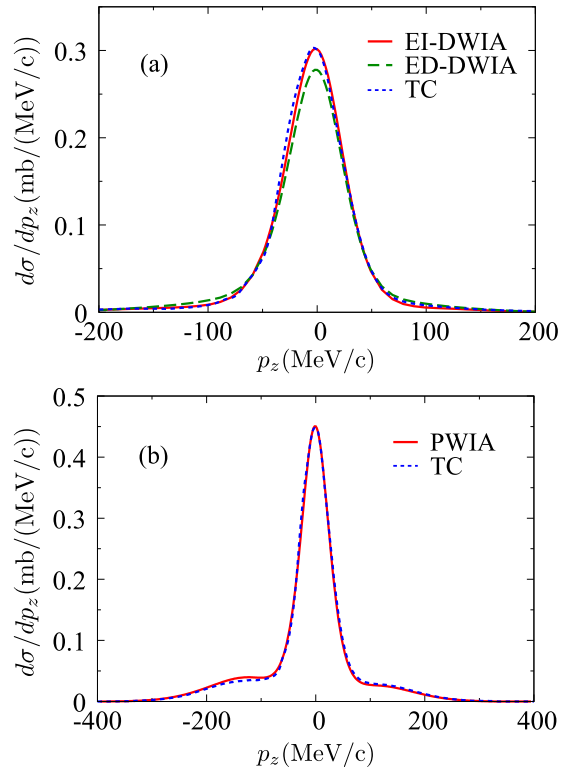

FIG. 1. (a) Longitudinal momentum distribution of the ^{15}C$(p,pn)^{14}$C reaction at 420 MeV/u. The struck neutron is assumed to be in a $2s$ orbital with a separation energy of 1.22 MeV. The solid, dashed, and dotted lines show the results of DWIA (energy-independent potentials), DWIA (energy-dependent potentials), and TC, respectively. (b) Same as (a) but with all distorting potentials switched off.

B. Comparison between TC and DWIA

In Fig. 1(a) we compare the longitudinal momentum distribution calculated with the DWIA and TC reaction frameworks. A separation energy of $S_n = 1.22$ MeV is assumed for the removed neutron in ^{15}C. For the nucleon-nucleus distorting potentials we use the Dirac phenomenology [21]. For the incident proton, this potential was evaluated at 420 MeV, whereas for the outgoing nucleus the potential was evaluated at 210 MeV. It is seen that the TC and DWIA results are in excellent agreement, both in shape and magnitude. From this comparison, we conclude that these reaction formalisms yield fully consistent results at this energy.

In Fig. 1(b) the same comparison with (a) but without all distorting potentials are shown. It should be noted that the agreement in the plane wave limit is worth investigating because a difference between DWIA and TC may appear, since the distortion effects suppress the tail region of MD, as shown in Fig. 1(a) and 1(b). As a result, the perfect agreement is found in the plane wave limit as well.

Since the outgoing nucleons are expected to emerge with a broad range of energies, using optical potentials fixed at

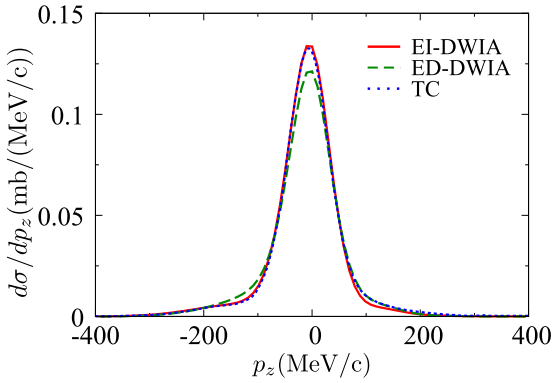

FIG. 2. Same as in Fig. 1(a) but for $S_n = 5$ MeV.

half of the incident energy may not be a good approximation. In DWIA, this effect can be readily taken into account by evaluating the outgoing distorted potentials at the energy given by their asymptotic momenta. To assess the importance of this effect, in Fig. 1(a) we show also the DWIA calculation including this energy dependence (dashed line).

One can see that, by taking the energy dependence of distorted waves into account, the LMD is reduced by 8.0% at the peak in the DWIA calculation so, at least for this system and incident energy, the energy dependence produces a minor, although non-negligible, effect.

C. Binding energy dependence

In this section we continue the benchmark test of DWIA and TC changing by the neutron separation energy artificially. In Figs. 2 and 3 LMD of ^{15}C$(p,pn)^{14}$C reaction with $S_n = 5$ MeV and 18 MeV are shown, respectively.

It is found that EI-DWIA, ED-DWIA, and TC also agree well in both $S_n = 5$ MeV and 18 MeV cases and at the same level as in the $S_n = 1.22$ MeV case. The LMD is reduced by 9.3% (4.9%) at the peak when $S_n = 5$ MeV (18 MeV) by taking the energy dependence of the optical potential parameters for the emitted p and n. It is also found that the asymmetric shape of LMD due to the asymmetry of the phase space, which is discussed in Ref. [23], is gradually developed as S_n increases through Figs. 1–3.

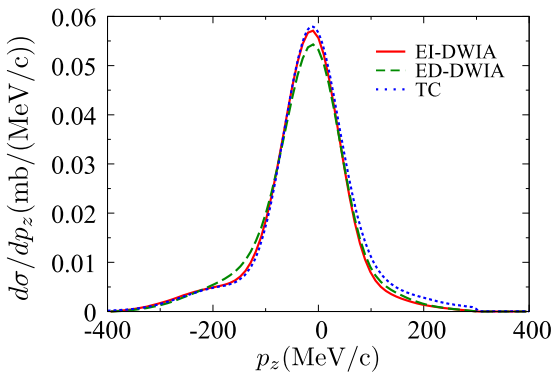

FIG. 3. Same as in Fig. 1(a) but for $S_n = 18$ MeV.

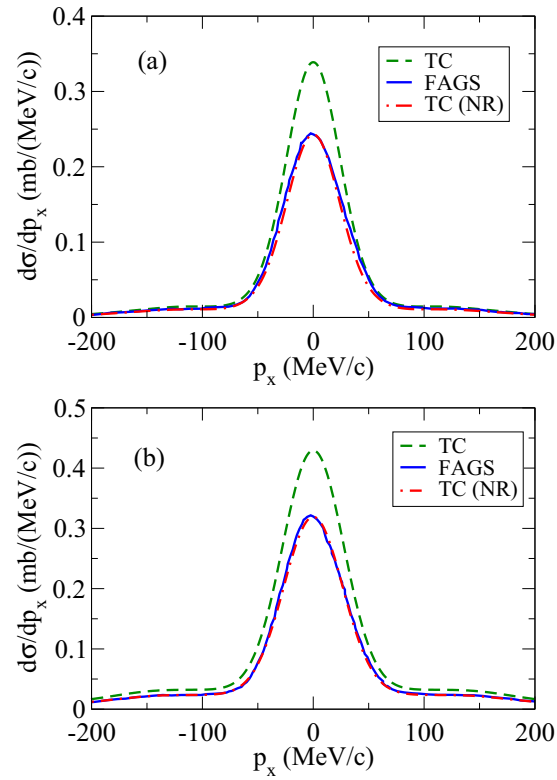

FIG. 4. (a) Transversal momentum distribution of ^{15}C$(p,pn)^{14}$C reaction at 420 MeV/u. The solid line is the FAGS result taken from Fig. 4 of Ref. [14]. The dashed and dot-dashed lines are the TC calculations with and without relativistic corrections, respectively. (b) Same as (a) but with all distorting potentials switched off.

D. Comparison with FAGS

Finally, we compare our calculations with the more sophisticated Faddeev-AGS (FAGS) framework. This in presented in Fig. 4, where we show the transverse momentum distribution for the ^{15}C$(p,pn)^{14}$C reaction at 420 MeV/u with $S_n = 1.22$ MeV. As in previous cases, the upper and bottom panels correspond to the full calculations and the calculations assuming plane waves for the incoming and outgoing nucleons. In each panel, the solid line is the FAGS calculation, taken from Fig. 4 of Ref. [14]. This calculation was performed with the Koning-Delaroche nucleon-nucleus potential, evaluated at 200 MeV, and assuming nonrelativistic kinematics. The dot-dashed line is the TC calculation using the same optical potential without any relativistic corrections for consistency. The agreement between these two calculations is excellent. It is to be noted that the FAGS calculation employs the CD-Bonn NN potential [24], whereas our TC implementation uses the Reid93 potential. These two NN potentials yield essentially the same on-shell observables up to 350 MeV, so we believe that, despite this different choice, the comparison is meaningful.

To highlight the importance of relativistic effects, we depict also in this figure the TC calculation including relativistic kinematics corrections (dashed line). It is seen that these corrections have a small effect on the shape of the momentum distribution, but they increase significantly its magnitude by about 30%.

Consequently, the inclusion of these relativistic effects will be relevant for the extraction of reliable spectroscopic factors from the analysis of (p,pn) data.

The same calculations shown in Fig. 4(a) but switching off the distorting potential of the incoming and outgoing nucleons are shown in Fig. 4(b) to see clearly the difference arising from a different choice of NN potentials. One can see that the good agreement between TC and FAGS remains in this case.

IV. SUMMARY

Transverse and longitudinal momentum distribution of the residual ^{14}C nucleus produced in the $^{15}\mathrm{C}(p,pn)^{14}\mathrm{C}$ knockout reaction at an incident energy of 420 MeV/u have been computed and compared using different reaction frameworks, namely, the distorted-wave impulse approximation (DWIA), the transfer-to-the-continuum (TC) method, and the Faddeev-AGS (FAGS) formalism.

The longitudinal momentum distributions evaluated with TC and EI-DWIA are found to be in excellent agreement both in the shape and magnitude. The agreement remains for increasing separation energies of the removed neutron, giving only 0.3%, 0.8%, 1.4% difference at the peak when $S_n = 1.22$ MeV, 5 MeV, 18 MeV, respectively, corroborating the consistency of the two methods for weakly bound and tightly bound systems. We found that the energy dependence of the optical potentials for emitted nucleons, which are not taken into account in TC, gives a minor, although non-negligible effect on knockout cross section.

The TC calculation, omitting relativistic kinematics corrections, is also found to reproduce remarkably well the FAGS calculation reported for this reaction. However, the inclusion of relativistic corrections increases the TC result by ∼30%, which highlights the relevance of these effects for the extraction of spectroscopic information from absolute (p,pN) cross sections.

From this study, we conclude that the DWIA and TC methods can be reliably used to analyze the momentum distributions for (p,pn) cross sections, which are currently being measured by several experimental campaigns. Extensions of the present benchmark to other situations, such as the $(p,2p)$ case or the removal from non s-wave nucleons, are in progress and will be published elsewhere.

ACKNOWLEDGMENTS

This work has received funding from the Spanish Ministerio de Economía y Competitividad under Project No. FIS2014-53448-C2-1-P and by the European Union Horizon 2020 research and innovation program under Grant Agreement No. 654002. M.G.-R. acknowledges support from the Spanish Ministerio de Educación, Cultura y Deporte, Research Grant No. FPU13/04109. A part of the computation was carried out with the computer facilities at the Research Center for Nuclear Physics, Osaka University. This work was supported in part by Grants-in-Aid of the Japan Society for the Promotion of Science (Grants No. JP16K05352 and JP15J01392), and RCNP Young Foreign Scientist Promotion Program.

[1] C. Samanta, N. S. Chant, P. G. Roos, A. Nadasen, J. Wesick, and A. A. Cowley, Phys. Rev. C **34**, 1610 (1986).
[2] N. S. Chant and P. G. Roos, Phys. Rev. C **15**, 57 (1977).
[3] C. Samanta, N. S. Chant, P. G. Roos, A. Nadasen, and A. A. Cowley, Phys. Rev. C **35**, 333 (1987).
[4] G. Jacob and Th. A. J. Maris, Rev. Mod. Phys. **38**, 121 (1966).
[5] G. Jacob and Th. A. J. Maris, Rev. Mod. Phys. **45**, 6 (1973).
[6] P. Kitching, W. J. McDonald, Th. A. J. Maris, and C. A. Z. Vasconcellos, Adv. Nucl. Phys. **15**, 43 (1985).
[7] T. Wakasa, K. Ogata, and T. Noro, Prog. Part. Nucl. Phys. **96**, 32 (2017).
[8] T. Aumann, C. A. Bertulani, and J. Ryckebusch, Phys. Rev. C **88**, 064610 (2013).
[9] L. D. Faddeev, Zh. Eksp. Teor. Fiz. **39**, 1459 (1960) [Sov. Phys. JETP **12**, 1014 (1961)].
[10] E. O. Alt, P. Grassberger, and W. Sandhas, Nucl. Phys. B **2**, 167 (1967).
[11] R. Crespo, A. Deltuva, E. Cravo, M. Rodríguez-Gallardo, and A. C. Fonseca, Phys. Rev. C **77**, 024601 (2008).
[12] R. Crespo, A. Deltuva, M. Rodríguez-Gallardo, E. Cravo, and A. C. Fonseca, Phys. Rev. C **79**, 014609 (2009).
[13] R. Crespo, A. Deltuva, and E. Cravo, Phys. Rev. C **90**, 044606 (2014).
[14] E. Cravo, R. Crespo, and A. Deltuva, Phys. Rev. C **93**, 054612 (2016).
[15] A. M. Moro, Phys. Rev. C **92**, 044605 (2015).
[16] M. Gómez-Ramos, J. Casal, and A. M. Moro, Phys. Lett. B **772**, 115 (2017).
[17] K. Yoshida, K. Minomo, and K. Ogata, Phys. Rev. C **94**, 044604 (2016).
[18] I. J. Thompson, Comput. Phys. Rep. **7**, 167 (1988).
[19] V. G. J. Stoks, R. A. M. Klomp, C. P. F. Terheggen, and J. J. de Swart, Phys. Rev. C **49**, 2950 (1994).
[20] R. V. Reid, Jr., Ann. Phys. (NY) **50**, 411 (1968).
[21] S. Hama, B. C. Clark, E. D. Cooper, H. S. Sherif, and R. L. Mercer, Phys. Rev. C **41**, 2737 (1990); E. D. Cooper, S. Hama, B. C. Clark, and R. L. Mercer, *ibid.* **47**, 297 (1993).
[22] A. J. Koning and J. P. Delaroche, Nucl. Phys. A **713**, 231 (2003).
[23] K. Ogata, K. Yoshida, and K. Minomo, Phys. Rev. C **92**, 034616 (2015).
[24] R. Machleidt, Phys. Rev. C **63**, 024001 (2001).